Supporting Information

Kumar et al. 10.1073/pnas.1014139107

SI Materials and Methods

Steady-State ATPase Activity Assay. ATPase activity of replication factor C (RFC) was assayed spectrophotometrically by using a phosphoenolpyruvate kinase–lactate dehydrogenase-coupled system. This assay measures the loss of NADH absorbance at 340 nm ($\varepsilon_M = 6250\ cm^{-1}\ M^{-1}$) as ADP is converted to ATP through the coupled action of pyruvate kinase and lactate dehydrogenase in the presence of phosphoenolpyruvate (1). The ATPase activity was determined at 25 °C in an assay solution containing 250 nM RFC, 250 nM proliferating cell nuclear antigen (PCNA) (K107C) or 5-[2(acetyl) aminoethyl] aminonaphthalene-1-sulfonate (AEDANS)-PCNA or Cy5-PCNA, 250 nM forked DNA, 1 mM ATP, 4 mM phosphoenolpyruvate, 360 μM NADH, and 4 units of phosphoenolpyruvate kinase–lactate dehydrogenase mix. The initial rates of ATP hydrolysis are reported.

Labeling of Mutant PCNA. The mutant PCNA (K107C) was labeled with Cy5 in a similar manner as described previously for labeling with AEDANS dye (2). The mutant PCNA was dialyzed against 20 mM Tris · HCl (pH 7.4) with 0.2 M NaCl and 10% glycerol. A 10-fold molar excess of Cy5-maleimide (GE Healthcare) was added to the mutant PCNA protein solution at 150 μM monomer concentration. The labeling reaction was allowed to proceed for 2 h at room temperature. The labeled PCNA was separated from the free Cy5 dye by size exclusion chromatography using a FPLC Superdex™ 200 column. The labeling efficiency of the mutant PCNA was determined by measuring the Cy5-dye concentration at 649 nm ($250{,}000\ M^{-1}\ cm^{-1}$). The PCNA concentration was determined by Bradford assay with wild-type yeast PCNA as standard. PCNA monomer labeling efficiency was 36.5%. According to this labeling efficiency, 59.3% of the labeled PCNA trimer is singly labeled, 34.1% is doubly labeled, and 6.54% is triply labeled. In single-molecule measurements, we can easily recognize the singly labeled species based on their single-step photobleaching or ∼0.8 FRET level of the high FRET state as compared to the near unity FRET (∼1.0) from doubly or triply labeled species. Only a singly labeled species was included in the data analyses.

Stoichiometry of PCNA:DNA. Cy5-labeled PCNA (250 nM) was loaded on Cy3-labeled DNA (100 nM) in the presence of RFC (400 nM) and ATPγS (5 mM) in the loading buffer. The reaction was carried out at room temperature for 5 min and loaded on a 0.2 mL monomeric avidin-agarose column (Pierce). The unbound PCNA was removed by addition of 10 mL of the buffer and PCNA:DNA complex then was eluted with 2 mM Biotin buffer. Eluate was applied to a PVDF membrane using a vacuum manifold device (BioRad). Cy3-DNA and Cy5-PCNA standards were blotted alongside on the membrane to generate a calibration curve of concentration versus fluorescence signal. The membrane was scanned on the laser-based scanner, Typhoon (GE Healthcare) and the amounts of PCNA and DNA were quantified using ImageQuant software.

Steady-State Fluorescence. Steady-state fluorescence spectroscopy was measured on a Jobin Yvon FluoroMax-4 fluorimeter. The buffer solution contained 25 mM Tris · HCl (pH 7.5), 10 mM $Mg(OAc)_2$, 100 mM NaCl, 0.05% ampholyte, and 1 mM DTT. The assay solution typically contains 250 nM Cy5-labeled PCNA mutants and 250 nM RFC equilibrated at 25 °C. To this solution, 5 mM ATP or ATPγS, 250 nM forked-DNA, and 250 nM streptavidin were sequentially added, and fluorescent spectra were taken after each addition with 532 nm excitation.

Stopped-Flow Fluorescence Spectroscopy. Stopped-flow studies were performed on a Kintek stopped-flow machine equipped with a fluorescence detector. The PCNA loading experiments were performed by mixing RFC · PCNA · ATP in one syringe with DNA in the other syringe, unless stated otherwise. The loading and unloading were monitored by exciting the donor (Cy3) at 514 nm and following the resulting FRET signal using a 645 cutoff filter (Andover Corporation). The data traces presented here are an average of at least three runs and were fit to exponential equations using GraphPad Prism 5. Conditions for each experiment are detailed in the figure captions.

Real-Time Single-Molecule Fluorescence Measurements. We used PEG-coated quartz microscope slides to monitor fluorescence signals from single Cy3 and Cy5 fluorophores. Cy3 attached forked-DNA substrate was immobilized on a quartz slide through biotin–streptavidin interaction. The RFC · PCNA complex in the presence of ATP or ATPγS was delivered into the channel containing the DNA substrate. Cy3-labeled forked-DNA substrate was excited with a 532-nm laser in a prism-coupled total internal reflection geometry and resonant energy transfer to Cy5 fluorescence signal was collected with a 1.2 N.A. 60× water immersion objective (Plan Apo; Nikon) in a custom total internal reflection geometry based on a commercial inverted microscope (TE2000; Nikon) with a 550-nm long-pass filter (Chroma) and a 650-nm long-pass dichroic mirror (Chroma). Fluorescence intensities from Cy3 and Cy5 were recorded simultaneously with an electron multiplying CCD camera (Cascade II; Roper Scientific) to obtain continuous FRET time traces in 35-ms time resolution until most of Cy3 photobleached. Glucose oxidase and catalase with 0.4% glucose in addition to Trolox was used to suppress blinking of dyes and to elongate dye photobleaching lifetimes (3). The laser power was controlled such that we have at least 3 min of Cy3 photobleaching lifetimes. These settings ensure that Cy5 intensity level change is mainly due to the PCNA loading dynamics, not to the blinking of Cy5.

Hidden Markov Model (HMM) Analysis. FRET time traces were analyzed with an HMM using a home-built HMM optimization code (4). Each set of traces per experimental settings was analyzed using two Gaussian distributions per state. This multiple Gaussian mixture model takes care of slight variations in the FRET values as FRET values can vary slightly due to day-to-day variations in the experimental conditions. Fig. 4 shows FRET values of the major components among the Gaussian mixture. In order to retrieve accurate information on the first binding event, the starting point of a trace was set to be either the point of PCNA · RFC · ATP injection, or the starting point of visually detectable nonzero FRET state. The FRET traces were also truncated at a time point of any faulty transitions caused by photobleaching or blinking of dyes to avoid overestimated rates.

1. Norby JG (1988) Coupled assay of Na^+, K^+-ATPase activity. *Methods Enzymol* 156:116–119.
2. Zhuang Z, Yoder BL, Burgers PM, Benkovic SJ (2006) The structure of a ring-opened proliferating cell nuclear antigen-replication factor C complex revealed by fluorescence energy transfer. *Proc Natl Acad Sci USA* 103:2546–2551.

3. Rasnik I, McKinney SA, Ha T (2006) Nonblinking and long-lasting single-molecule fluorescence imaging. *Nat Methods* 3:891–893.

4. Gomes X, Schmidt SL, Burgers PM (2001) ATP utilization by yeast replication factor C. II. Multiple stepwise ATP binding events are required to load proliferating cell nuclear antigen onto primed DNA. *J Biol Chem* 276:34776–34783.

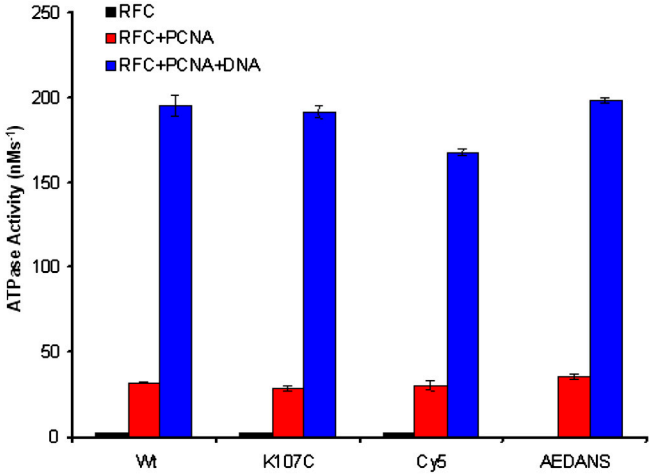

Fig. S1. Activities of labeled PCNA mutants in stimulating yeast RFC ATPase activity. The ATPase activity was determined at 25 °C in an assay solution containing 250 nM RFC, 250 nM PCNA, or Cy5-PCNA or AEDANS-PCNA, 250 nM Bio62/34/36-mer DNA, 1 mM ATP, 4 mM phosphoenolpyruvate, 360 μM NADH, and 4 units of phosphoenolpyruvate kinase–lactate dehydrogenase mix.

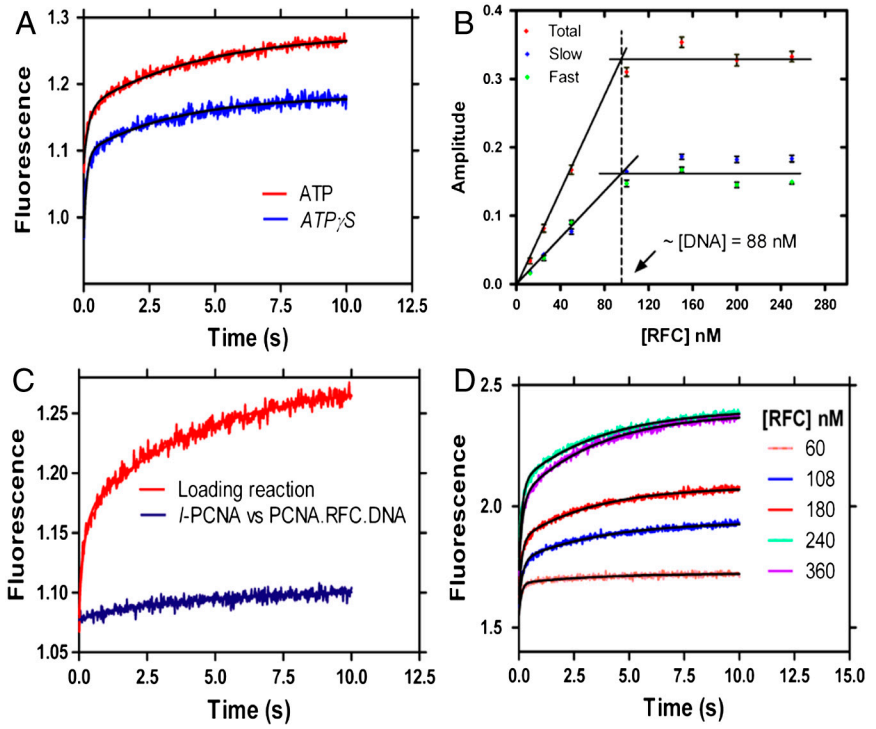

Fig. S2. PCNA loading in the presence of ATP and ATPγS. (*A*) The RFC · PCNA (200 nM concentration each) formed in the presence of ATP or ATPγS (5 mM) was mixed with DNA (200 nM) in a stopped-flow instrument and the FRET signal was followed at 665 nm. Extended time course traces showed two distinct phases; a fast phase with the rate constants of 7 ± 1 s^{-1} and 8 ± 1 s^{-1}, and a slow phase at the rate constants of 0.26 ± 0.04 s^{-1} and 0.29 ± 0.02 s^{-1}, respectively, for ATP and ATPγS. Additionally, the amplitude of the signal was $49 \pm 6\%$ with ATP and $52 \pm 6\%$ ATPγS. (*B*) The amplitudes from the fast and slow phases as function of RFC concentration. (*C*) Labeled PCNA (88 nM) was mixed with RFC · PCNA · DNA (in the ratio of 1 : 1 : 2 with concentration of RFC at 88 nM (note that the PCNA in this complex is unlabeled) in the presence of excess ATP and the FRET signal was followed at 665 nm. For comparison, loading of labeled PCNA on DNA (without unlabeled PCNA in this case) is shown in the red trace. The amplitude of the labeled PCNA (*I*-PCNA) loading in the presence of the preformed complex (RFC · PCNA · DNA) shown in the blue trace is less than 10% of the red trace. (*D*) Effect of RFC · PCNA ratio: The PCNA concentration (90, 140, 180, 260, and 400 nM) in these reactions was varied such that RFC · PCNA were in a 1 : 1 complex ($K_d = 1.3$ nM) (4). Varying levels of RFC · PCNA · ATP were mixed with DNA at 200 nM concentration and the FRET signal was followed at 665 nm. The data were fit to a double-exponential equation. The rate of the fast (7 ± 1 s^{-1}) and the slow (0.26 ± 0.04 s^{-1}) phases did not vary with the increasing PCNA concentration and agreed with those obtained from data in Fig. 2*A*.

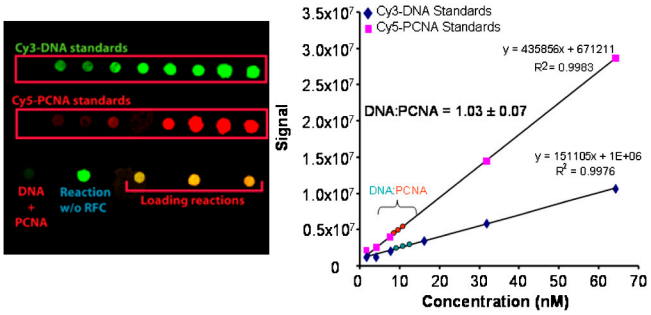

Fig. S3. Stoichiometry of RFC and PCNA on DNA. Dilutions of labeled DNA and PCNA were used as standards. Loading reactions (in triplicate) along with the controls without RFC and one with mix of DNA and PCNA were also blotted on a PVDF membrane and imaged on Typhoon 9400. The quantitation was done using ImageQuant software.

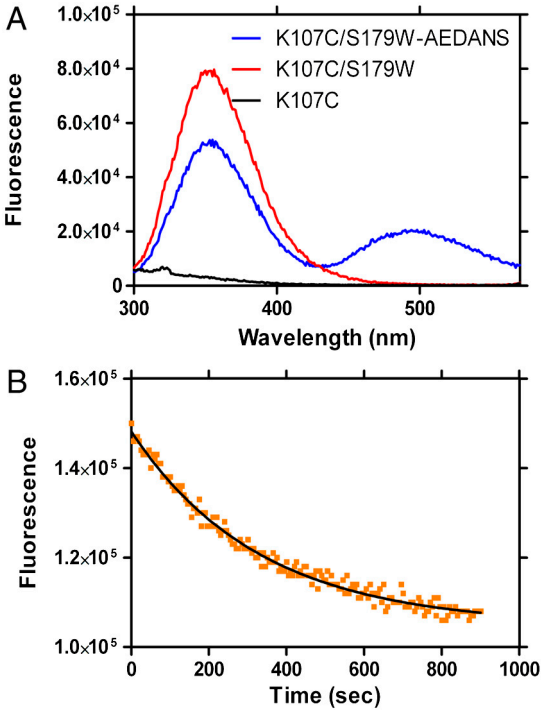

Fig. S4. Fluorescence emission spectra of the variants of the PCNA protein and PCNA subunit exchange. (*A*) Each emission spectrum was obtained using an excitation wavelength of 280 nm where K107C/S179W-AEDANS is a mutant PCNA with a FRET donor (W179) and acceptor (C107 AEDANS) pair, K107C/S179W is mutant PCNA with tryptophan without AEDANS, and K107C is mutant PCNA without dye and tryptophan. All protein concentrations were 200 nM. (*B*) The K107C/S179W-AEDANS PCNA was mixed against the K107C PCNA at 25 °C. The fluorescence emission resulting from excitation with 290 nm light was monitored at 488 nm and the data were fit to a single-exponential equation.

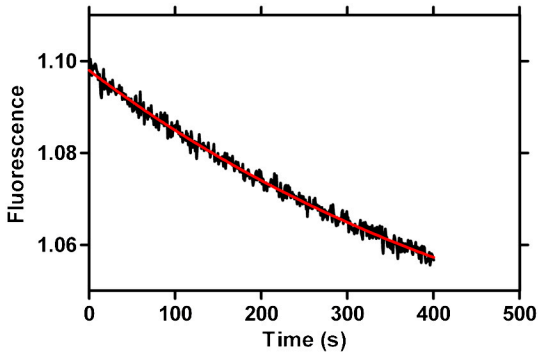

Fig. S5. Unloading of PCNA in the presence of ATPγS. Cy5-labeled PCNA (200 nM), RFC (200 nM), and Cy3-labeled forked-DNA was mixed in the presence of excess ATPγS (5 mM). This preformed RFC · PCNA · ATPγS complex was mixed with an excess of unlabeled PCNA (2 μM) in a stopped-flow instrument and FRET signal was followed at 665 nm. The loading traces were fit to a single-exponential equation with the rate constant of 0.004 s^{-1}.

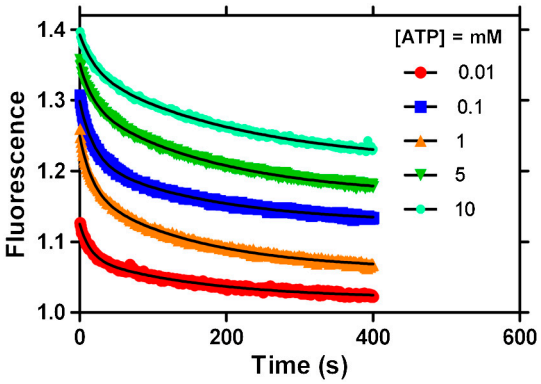

Fig. S6. PCNA loading is independent of ATP concentration. The RFC · PCNA · ATP (RFC and PCNA at 200 nM each) complex with varying concentrations of ATP (0.01–10 mM) was incubated with DNA (200 nM) for 5 min to ensure complete loading followed by rapid mixing with excess unlabeled PCNA to follow the disassembly of the PCNA from the complex. At all the concentrations of ATP, we observed the two phases of 0.05 ± 0.01 s^{-1} for the fast phase and 0.005 ± 0.001 s^{-1} for the slow phase with relative amplitudes of 38 ± 9 and 62 ± 9, respectively. The amplitudes of the two phases were reduced at lower concentrations of ATP (<1 μM), most likely due to partial loading.

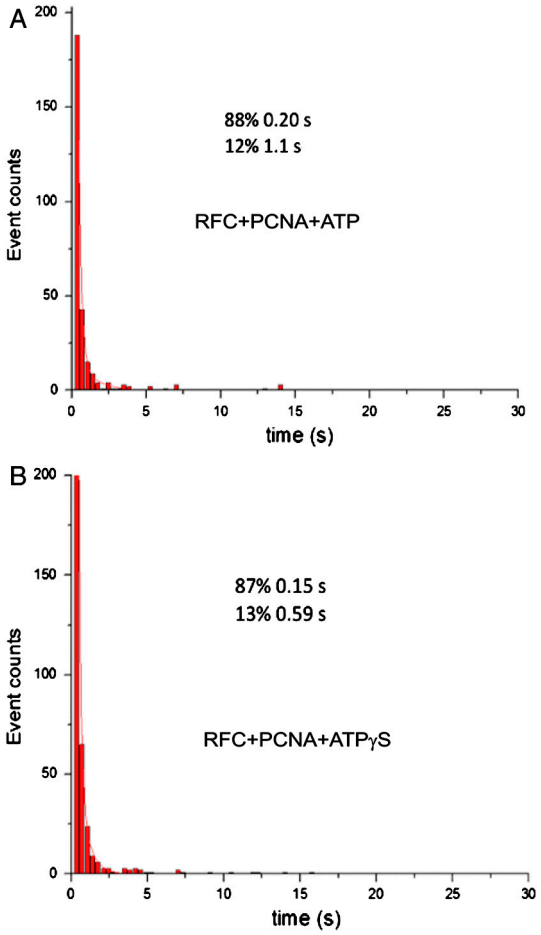

Fig. S7. Lifetime distribution of the highest FRET state in two cases. The histograms were constructed by visual inspection of FRET traces. The histograms are well fitted with double-exponential decay. The lifetime measured for the longer living component is significantly shortened by the uncertainty associated with arbitrary visual inspection, dye photobleaching, and blinking. Nevertheless, double-exponential decay is evident in both cases. The lifetimes and population ratios of the double-exponential components are displayed in the charts. The short-lifetime component is assigned to the transient conformation (the off-path RFC · ATP · PCNA · DNA^{+} state in Fig. 4*D*) and the long-lifetime component includes the stably loaded PCNA conformation (RFC · ATP · PCNA · DNA^{*}), and a transient PCNA conformation (RFC · ATP · PCNA · DNA″) as in Fig. 4*D*. (*A*) PCNA loaded on DNA in the presence of RFC and ATP. (*B*) PCNA loaded on DNA in the presence of RFC and a nonhydrolyzable ATP analog ATPγS.

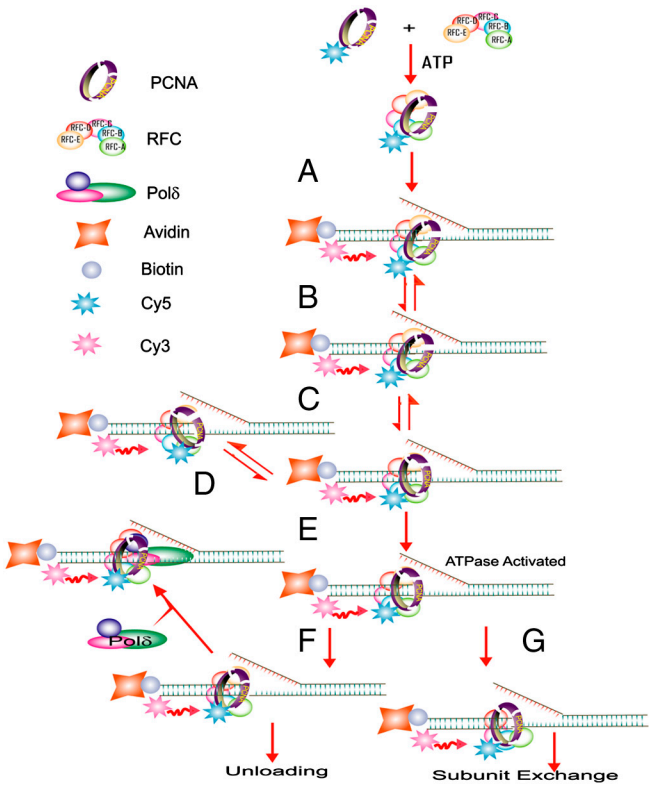

Fig. S8. Model for PCNA loading on the DNA. This model is based on ensemble kinetics and single-molecule FRET studies: (*A*) The RFC binds to the PCNA in the presence of ATP, a conformational change in RFC results in opening of the PCNA subunit interface without hydrolyzing the ATP. The PCNA · RFC · ATP complex rapidly binds DNA. (*B*) The PCNA · RFC · ATP · DNA complex undergoes a fast conformational change. (*C*) The PCNA · RFC · ATP · DNA complex undergoes a second conformational change. (*D*) A transient unstable species is formed that does not continue to a competent complex. (*E*) An ATPase activated state of the RFC · PCNA · DNA complex that partitions to two stable complexes. (*F* and *G*) Loaded PCNA exists in two subpopulations and is unloaded either by subunit exchange or dissociates with RFC from the DNA. In the presence of polymerase δ (polδ) only one of the two species converts to the RFC · PCNA · DNA · polδ holoenzyme.

Table S1. PCNA subunit exchange rate constants

Reactions	Trap	$k_{exchange}$,* s^{-1}
250 nM AED-PCNA †	2.5 μM PCNA	0.0023 ± 0.0003
250 nM AED-PCNA, 250 nM RFC, and 5 mM ATP	2.5 μM PCNA	0.0013 ± 0.0006
250 nM AED-PCNA, 250 nM RFC, 250 nM Bio15/45/33 DNA, and 5 mM ATP	2.5 μM PCNA	0.0029 ± 0.0006

*Values represent rate constants extracted from a single-exponential function.
†AED-PCNA represents the PCNA-K107C-AEDANS-S179W and trap PCNA (PCNA without AEDANS and S198W).